ตำแหน่ง X ช่องว่างแถบพลังงานของ Si<Sn<Ge เมื่อเราเติมซิลิกอนลงไปในโลหะผสม $Ge_{(1-x-y)}Si_xSn_y$ จะมีช่องว่างแถบพลังงานเพิ่มขึ้นเนื่องจากสารตั้งต้นของเรามีช่องว่างแถบพลังงานน้อยที่สุดในทำนองเดียวกันเมื่อเติมดีบุกลงไปก็จะทำให้ช่องว่างแถบพลังงานที่ตำแหน่งนี้เพิ่มขึ้นตามด้วย

ความเป็น Direct band gap ของโลหะผสม $Ge_{(1-x-y)}Si_xSn_y$ โดยการเปรียบเทียบแถบสีช่องว่างแถบพลังงานที่ตำแหน่ง L ตำแหน่ง Γ และตำแหน่ง X ค่า x และ y ใดบ้างที่ทำให้ตำแหน่ง Γ มีค่าน้อยกว่าตำแหน่ง L และ X ถือว่าตำแหน่งนั้นมีความเป็น direct band gap นำค่าที่ได้มาเขียนกราฟได้ดังรูปที่ 4-16

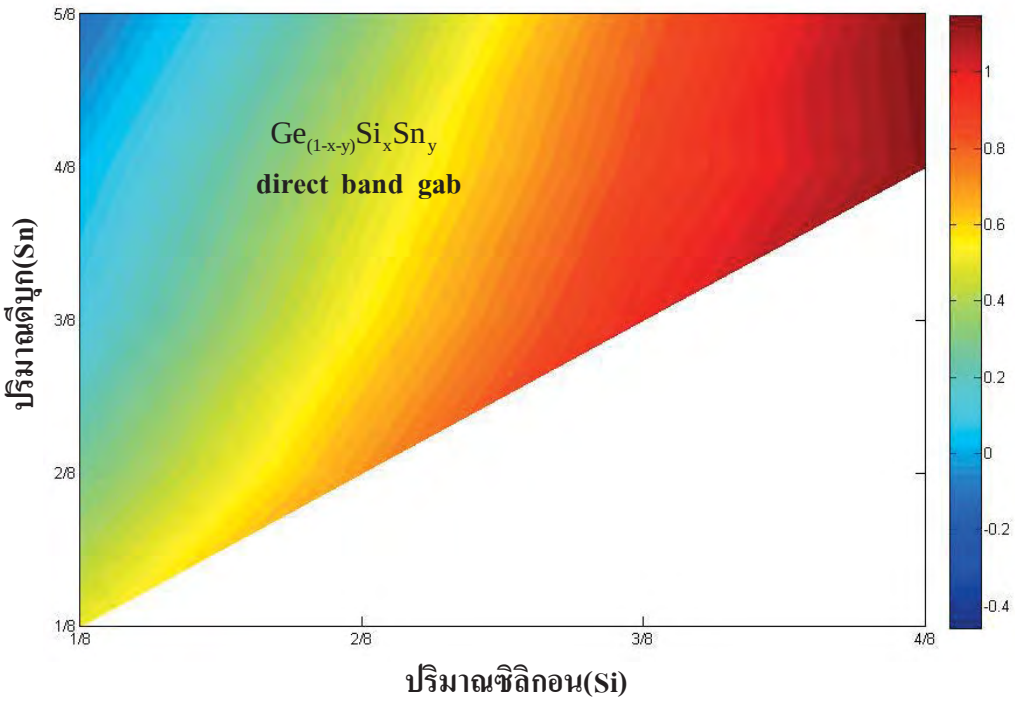

รูปที่4-16 ช่องว่างแถบพลังงานของ $Ge_{(1-x-y)}Si_xSn_y$ โดยแบบจำลอง VCA

เราจะได้ความเป็น Direct band gap ของ $Ge_{(1-x-y)}Si_xSn_y$ ในบริเวณที่เป็นแถบสีดังแสดงในรูปที่ 4-35 ซึ่งความเป็น direct band gap ซึ่งมีค่าตั้งแต่ 0-1 eV ของโลหะผสมนี้สามารถปรับค่าได้ขึ้นอยู่กับปริมาณของซิลิกอน เจอมิเนียม และดีบุก ที่อยู่ในโลหะผสม และสามารถที่นำไปประยุกต์ใช้ในอุปกรณ์อิเล็กทรอนิกส์ได้หลายด้านขึ้นกับค่าช่องว่างแถบพลังงานที่ต้องการ

4.2.2 การคำนวณโดยใช้แบบจำลอง Mixed atoms

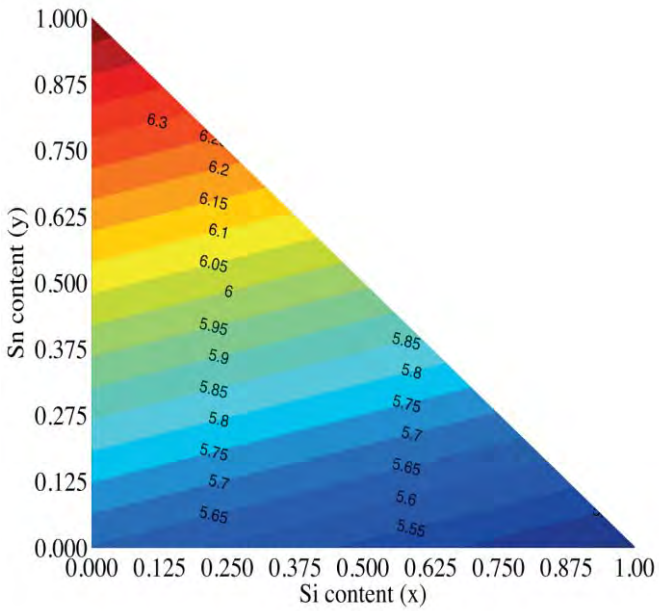

รูปที่ 4-16 ค่าคงที่แลททิซของโลหะผสม $Ge_{1-x-y}Si_xSn_y$ โดยการประมาณแบบ Vergard law

จากการใช้แบบจำลองแบบ super-cell ในการคำนวณสมบัติทางอิเล็กตรอนของโลหะผสม $Ge_{1-x-y}Si_xSn_y$ ที่ทำการสังเคราะห์บนวัสดุรองรับ CeO_2 เราพบว่าตัวแปรที่สำคัญสำหรับการที่จะทำให้โลหะผสมที่ได้มีลักษณะเป็นสารกึ่งตัวนำชนิดแถบพลังงานตรงนั้นคือปริมาณ ของประกอบของโลหะผสมและความเครียดอันเนื่องความแตกต่างของค่าคงที่แลททิซของตัวโลหะผสมและตัววัสดุรองรับ ดังแสดงในรูปที่ 4.16 และ 4.17

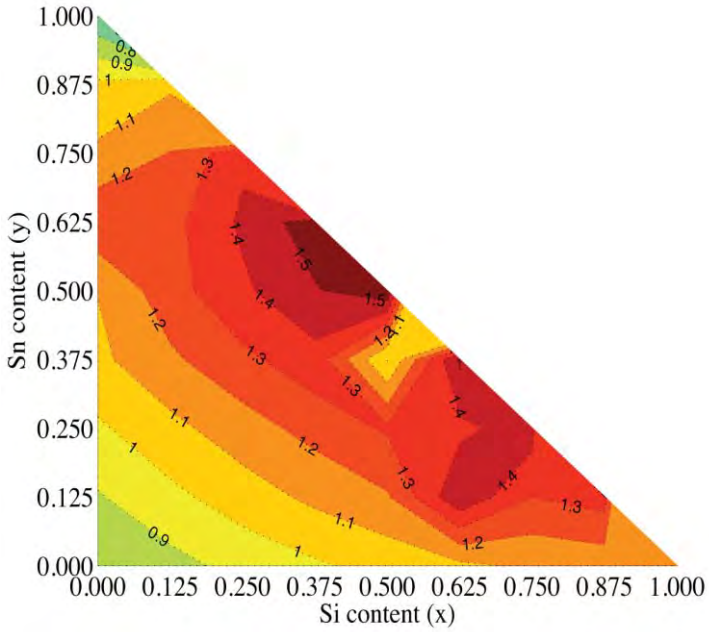

(ก)

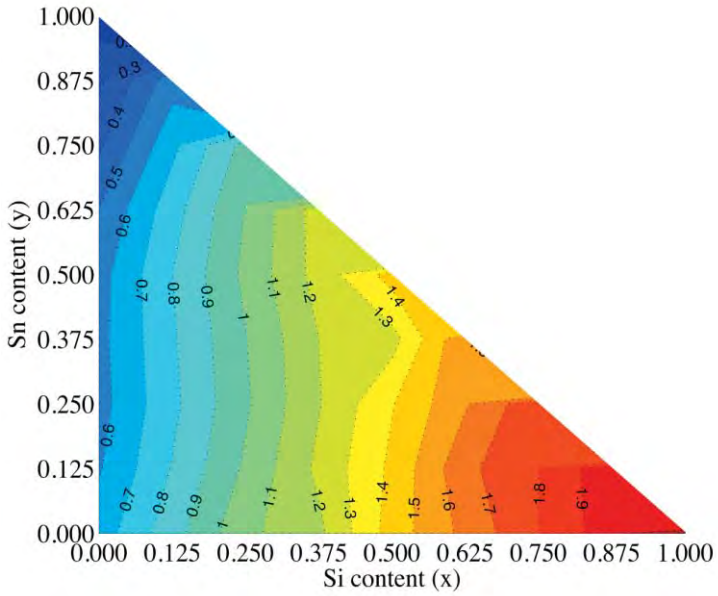

(ข)

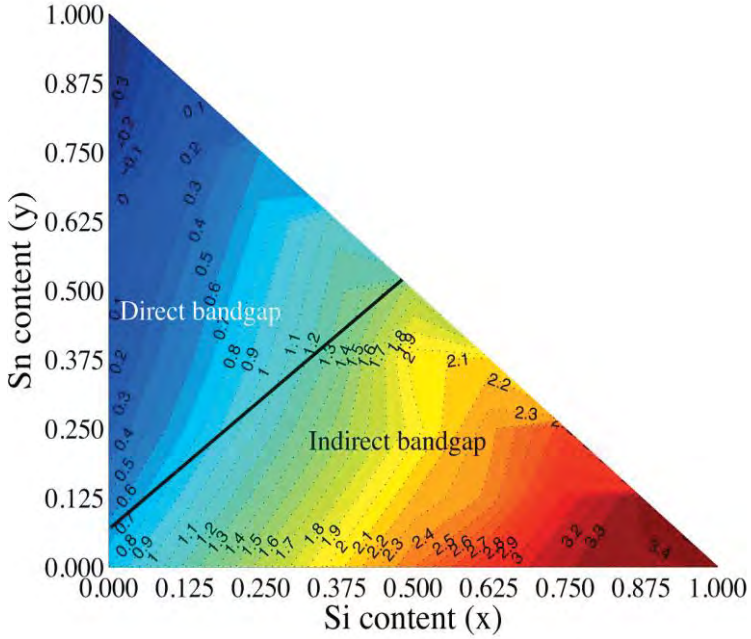

(ค)

รูปที่ 4-17 แถบสีความกว้างแถบพลังงานโดยใช้แบบจำลอง Mixed atoms ที่ตำแหน่ง (ก) X valley (ข) L valley และ (ค) ที่จุด Γ

บทที่ 5
บทสรุป

5.1 สรุป

ในการศึกษาผลของช่องว่างของออกซิเจนที่มีต่อโครงสร้างของ CeO_2 บริสุทธิ์ และโครงสร้างของ $A_xCe_{1-x}O_2$ ที่เจือด้วย C Fe Mn และ Co โดยใช้วิธี Density Function Theory (DFT) โดยใช้ LSDA+U สำหรับโครงสร้างที่ศึกษาได้ผลสรุปคือ เมื่อพิจารณาความหนาแน่นสถานะและค่าพลังงานพบว่า CeO_2 บริสุทธิ์มีค่าช่องว่างพลังงานที่ทำการคำนวณได้ 2.71 eV ซึ่งจากการทดลองของ Maensiri และคณะ(Santi Maensiri C. M., 2007) มีค่าช่องว่างแถบพลังงาน 3.57 eV - 3.61 eV จะเห็นได้ว่าการคำนวณในรายงานนี้มีค่าต่ำกว่าค่าที่ได้จากการทดลอง เนื่องจากการเลือกใช้วิธี DFT และผลการวิเคราะห์ความหนาแน่นสถานะสำหรับโครงสร้างที่เจือด้วยธาตุ C Fe Mn และ Co พบว่ามีสถานะของอิเล็กตรอนที่เจือและมีช่องว่างพลังงานลดลง ศึกษาผลของช่องว่างของออกซิเจนที่มีต่อโครงสร้างของ CeO_2 บริสุทธิ์พบว่า CeO_2 บริสุทธิ์มีสมบัติแบบแอนติเฟอร์โร เนื่องจากการเกิดอันตรกิริยาแบบ Super exchange เมื่อมีการนำเอาออกซิเจนออกจากโครงสร้างของCeO_2 จะเกิดอันตรกิริยาแบบ F-centre exchange ที่มีช่องว่างของออกซิเจนเป็นตัวกลางในการเกิดการควบคู่แบบเฟอร์โรแมกเนติก พบว่ามีสถานะของอิเล็กตรอนที่เจือและมีช่องว่างพลังงานเล็กๆ เกิดขึ้นภายในบริเวณแถบช่องว่างพลังงานหรือเกิดเป็น intermediate band

จากการคำนวณโครงสร้างแถบพลังงานของโลหะผสม $Ge_{(1-x-y)}Si_xSn_y$ ที่แสดงคุณสมบัติเป็น direct band gap ด้วยโปรแกรม ABINIT และโปรแกรมที่พัฒนาขึ้น พบว่าโปรแกรม ABINT คำนวณคุณสมบัติโครสร้างแถบพลังงานของซิลิกอน มีช่องว่างแถบพลังงานเท่ากับ 0.55 eV ซึ่งค่าแตกต่างจากทฤษฎีมากจึงไม่นำโปรแกรม ABINIT คำนวณคุณสมบัติของธาตุตัวอื่นต่อไป และใช้โปรแกรมที่พัฒนาขึ้นคำนวณคุณสมบัติต่างๆทั้ง โครงสร้างแถบพลังงาน ความหนาแน่นอิเล็กตรอน ความหนาแน่นสถานะและจำนวนสถานะ ที่มีค่าใกล้เคียงกับทฤษฎีผลการคำนวณโครงสร้างแถบพลังงานที่เป็น direct band gap ของ $Ge_{(1-x-y)}Si_xSn_y$ ใช้แบบจำลองแบบ Virtual Crystal Approximation (VCA) และแบบ mixed atoms มีค่าตั้งแต่ 0-0.8 eV ขึ้นกับปริมาณของซิลิกอน เจอมิเนียม และดีบุก ที่อยู่ในโลหะผสม และสามารถที่นำไปประยุกต์ใช้ในอุปกรณ์อิเล็กทรอนิกส์ได้หลายด้านขึ้นกับค่าช่องว่างแถบพลังงานที่ต้องการ

เอกสารอ้างอิง

J. R. Chilikowsky, and M. L. Cohen (1976), Phys. Rev. B **14**,556.

J.M.D. Coey, A. D. (2004). Ferromagnetism in Fe-doped SnO2 thin films. *Applied Physics Letter* (84), 1332-1334.

J.M.D. Coey, V. M. (2005). Donor impurity band exchang in dilute ferromagnetic oxides. *NaturebMaterials* (4), 173-179.

M. V. Fischetti and S. E. Laux (1996), Juournal of Apptied Physics 80, 2234

Mogens Mogensen, *. T. (1994). Solid Oxide Fuel Cell Anodes of Doped CeO2. *8* (141), p. 2122.

N.V.Skorodumova, S. B. (2002). Quantum Origin of the Oxygen Storage Capability of Ceria. *Physics Review Letters , 16* (89), p. 166601.

P. Harrison (2005). Quantum wall wires and dots : theoretical computational physics., Chichester : wiley.

P. Moontragoon, Z. Ionic, and P.Harison (2007), “Band structure calculation of SiGeSn alloy: achieving direct band gap materials”, Semicond. Sci Technol. **22**, 742

Qi-Ye Wen, H.-W. Z.-Q.-H. (2007). Room-temperature ferromagnetism in pure and Co doped CeO2 powders. *Journal of Physics: Condensed Matter* (19), p. 246205.

R. Ragan (2002). Direct Energy band gap group IV Alloys and nanostructure Dissertation., California Institute of technology.

S.Tsunekawa, R. a. (2000). Origin of the Blue Shift in Ultraviolet Absorption Spectra of Nanocrystalline CeO2-x Particles. *Materials Transaction-JIM* (41), pp. 1104-1107.

Santi Maensiri, C. M. (2007). Egg White Synthesis and Photoluminescence of Platelike Clusters of CeO2 Nanoparticles. *Crystal Growth & Design , 5* (7), 950.

Santi Maensiri, S. P. (2009). Room temperature ferromagnetism in Fe-doped CeO2 nanoparticles. *Journal of Nanoscience and Nanotechnology , 11* (9), 6415-6420.

Slusser, P. K. (2009). *TRANSITION METAL DOPED CERIUM OXIDE FOR SPINTRONICS APPLICATIONS.* Utah: University of Utah.

Song, Y. (2007). Room-Temperature Ferromagnetism of Co-Doped CeO2 Thin Films on Si(111) substrates. *Chinese Physics Letters* (24), pp. 218-221.

Spaldin, N. A. (2003). *Magnetic matterials:fundamenals and device applications.* United Kingdom: Cambridge.

Tiwari, A. B. (2006). Ferromagnetism in Co doped CeO2: Observation of a giant magnetic moment with a high Curie temperature. *Applied Physics Lettera* (88), p. 142511.

W.J.Thomus, J. T. (1997). *Principles and practice of heterogrneous catalysis.* New York: Vancouver Coastal Health.

Wang, Q. (2003). *ANODIC ELECTROCHEMICAL SYNTHESIS AND CHARACTERIZATION OF NANOCRYSTALLINE CERIUM OXIDE AND CERIUM OXIDE / MONTMORILLONITE NANOCOMPOSITES.* Texas: University of North Texas.

ไพโรจน์ มูลตระกูล. (2551). *Computational Materials Science.* ขอนแก่น: ภาควิชาฟิสิกส์ คณะวิทยาศาสตร์ มหาวิทยาลัยขอนแก่น.

พิมพ์สวัสดิ์, อ. (2553). *การคำนวณโครงสร้างอิเล็กทรอนิกส์และสมบัติแม่เล็กของนิเกิลออกไซด์บริสุทธิ์และที่เจือด้วยโลหะทรานซิชันบางตัว.* มหาวิทบาลัยขอนแก่น.

สุมาลินทร์ พ่อค้า. (2551). *ออกไซด์เจือแม่เหล็กของอนุภาคนาโนกลุ่ม CeO2 : การสังเคราะห์ การศึกษาลักษณะเฉพาะ และสมบัติทางแม่เหล็ก.* ขอนแก่น: ภาควิชาฟิสิกส์ คณะวิทยาศาสตร์ มหาวิทยาลัยขอนแก่น.

อินทร์เจริญ, พ. พ. (2551, กรกฎาคม). Preparation of Cerium Oxide Nanoparticles by Microemulsion Method. *วารสารวิจัย มข. , 6* (13), p. 638.

ภาคผนวก

ARTICLE IN PRESS
NOC-15877; No of Pages 3

Journal of Non-Crystalline Solids xxx (2012) xxx–xxx

Contents lists available at SciVerse ScienceDirect

Journal of Non-Crystalline Solids

journal homepage: www.elsevier.com/locate/jnoncrysol

Electronic properties calculation of $Ge_{1-x-y}Si_xSn_y$ ternary alloy and nanostructure

Pairot Moontragoon [a,*], Pichitpon Pengpit [a], Thanusit Burinprakhon [a], Santi Maensiri [b], Nenad Vukmirovic [c], Zoran Ikonic [d], Paul Harrison [d]

[a] Department of Physics, Faculty of Science, Khon kaen University, Khon kaen, 40002, Thailand
[b] School of Physics, Suranaree University of Technology, Nakhon Ratchasima 30000, Thailand
[c] Institute of Physics, University of Belgrade, Serbia
[d] School of Electronic and Electrical Engineering, University of Leeds, Leeds, United Kingdom

ARTICLE INFO

Article history:
Received 10 September 2011
Received in revised form 1 January 2012
Available online xxxx

Keywords:
Silicon photonic devices;
SiGeSn alloys;
Direct band gap semiconductor

ABSTRACT

The band structure of $Ge_{1-x-y}Si_xSn_y$ ternary alloys, which are easier to grow than binary $Ge_{1-x}Sn_x$ alloys, and clearly offer a wider tunability of their direct band-gap and other properties, was calculated and investigated by using the empirical pseudo-potential plane wave method with modified Falicov pseudo-potential formfunction. The virtual crystal approximation (VCA) and $2\times2\times2$ super-cell (mixed atoms) method were adopted to model the alloy. In order to calculate all of these properties, the empirical pseudo-potential code was developed. The lattice constant of the alloy varies between 0.543 to 0.649 nm. The regions in the parameter space that corresponds to a direct or indirect band gap semiconductor are identified. The $Ge_{1-x-y}Si_xSn_y$ ternary alloy shows the direct band gap for appropriate composition of Si, Ge and Sn. The direct energy gap is in the range 0–1.4 eV (from the VCA calculation), and 0–0.8 eV (from the super-cell calculation), depending on the alloy composition. Therefore, this alloy is a promising material for optoelectronic applications in both visible and infrared range, such as interband lasers or, solar cells. Furthermore, strain-free heterostructures based on such alloys are designed and, using the effective-mass Hamiltonian model, the electronic structure of GeSiSn quantum wells with arbitrary composition is investigated, in order to understand their properties and the potential of their use in devices.

1. Introduction

SiGeSn alloys have attracted research attention as promising materials for optoelectronic applications [1–3], such as interband lasers, detectors, and solar cells, because they may be direct bandgap semiconductors, and fully compatible with Si-based technology. They have the potential for independent variation of the band structure and lattice constant and can be used in both lattice-matched and strained layer structures. Offering the possibility of emission and absorption in the visible, near- and mid-IR range, they have the prospect of applications for solar cell, photodetectors, electro-absorption and electro-optic modulators, etc.

2. Computational details

For band structure calculation of $Ge_{1-x-y}Si_xSn_y$ alloys when x and y were varied from 0 to 0.4, we used the empirical pseudo-potential plane wave method, which can predict the band structure and optical properties of semiconductors with good accuracy. The calculations for alloys were made both within the virtual crystal approximation and by the super-cell (mixed atom) method, using the available experimental data for comparison. The modified Falicov pseudo-potential formfunction was adopted [4], as given by Eq. (1),

$$V(\mathbf{q}) = \left[b_1\left(\mathbf{q}^2-b_2\right)/\left[2\left(1+exp\left(b_3\left(\mathbf{q}^2-b_4\right)\right)\right)\right]\times\left[tanh\left(\left(b_5-\mathbf{q}^2\right)/b_6\right)+1\right] \quad (1)$$

where the parameters b_1, b_2, b_3, b_4, b_5 and b_6 for silicon, germanium and gray tin are given in Table 1, and $\mathbf{q}$ is the wave vector (in atomic units).

3. Results

The lattice constant of $Ge_{1-x-y}Si_xSn_y$ alloy was calculated by using the Vegard's law [5,6] with the bowing correction, by using quadratic interpolation of lattice constants of silicon, germanium and gray tin, as given by Eq. (2),

$$a_{GeSiSn} = a_{Ge} + \Delta_{SiGe}(x) + \theta_{SiGe}(x)(1-x) + \Delta_{SnGe}(y) + \theta_{SnGe}(y)(1-y), \quad (2)$$

where a_{Ge}, a_{Si}, and a_{Sn} are the lattice constants of germanium, silicon and gray tin, respectively, and Δ_{SiGe} (Δ_{SnGe}) denote $a_{Si}-a_{Ge}$ ($a_{Sn}-a_{Ge}$), respectively. The bowing parameter for lattice constant of $Ge_{1-x}Si_x$, θ_{SiGe}, is −0.026 and that of $Ge_{1-y}Sn_y$, θ_{GeSn}, is 0.166. The alloy lattice

* Corresponding author.
E-mail address: mpairo@kku.ac.th (P. Moontragoon).

0022-3093/$ – see front matter © 2012 Elsevier B.V. All rights reserved.
doi:10.1016/j.jnoncrysol.2012.01.025

Please cite this article as: P. Moontragoon, et al., Electronic properties calculation of $Ge_{1-x-y}Si_xSn_y$ ternary alloy and nanostructure, J. Non-Cryst. Solids (2012), doi:10.1016/j.jnoncrysol.2012.01.025

Table 1
The parameters of the modified Falicov pseudo-potential for silicon, germanium and gray tin.

Parameter	b_1	b_2	b_3	b_4	b_5	b_6
Si	0.3969	2.2286	0.6120	−1.9620	5.0	0.3
Ge	0.4229	2.4682	0.6060	−2.6260	5.0	0.3
α-Sn	0.4199	2.1600	0.6407	−2.9820	5.0	0.3

constant dependence on the composition x and y is shown in Fig. 1. Due to the lack of any data on quadratic terms for the empirical pseudo-potential formfunction of the alloy for the VCA based calculations, this was calculated in the same manner, but only with linear interpolation,

$$V_{GeSiSn} = V_{Ge}(1-x-y) + V_{Si}(x) + V_{Sn}(y), \quad (3)$$

where V_{Ge}, V_{Si}, and V_{Sn} are the empirical pseudo-potentials of germanium, silicon and gray tin, respectively. The VCA is known to give an almost linear dependence of the direct gap of GeSn on the Sn mole fraction, while there exists a significant bowing [7]. Moreover, the exact arrangement of Ge, Si and Sn atoms (any ordering or clustering) will significantly affect the band gap properties. Therefore, in order to check the accuracy of the VCA for the random alloy, the super-cell (mixed atom) method was also employed, with 2×2×2 crystalline cubic cells (64 atoms) in the super-cell. The $Ge_{1-x-y}Si_xSn_y$ alloy is obtained by randomly distributing X = 64x Si atoms, Y = 64y Sn atoms, and 64-X-Y Ge atoms over the 64 lattice sites of the super-cell. The band structure of the random alloy is obtained by averaging the results over a significant numbers of possible configurations. We should also note that random alloys may be considered by the elegant technique of special quasirandom structures [8], with atomic configuration within the limited-size super-cell constructed so to maximally mimic the randomness of the alloy, and a single super-cell calculation, rather than averaging over a number of them, suffices. However, only a small number of composition combinations in ternary alloys leads to relatively small special quasirandom super-cells [9], and in order to cover a more dense mesh of alloy compositions we have here used multiple random configurations and averaging. According

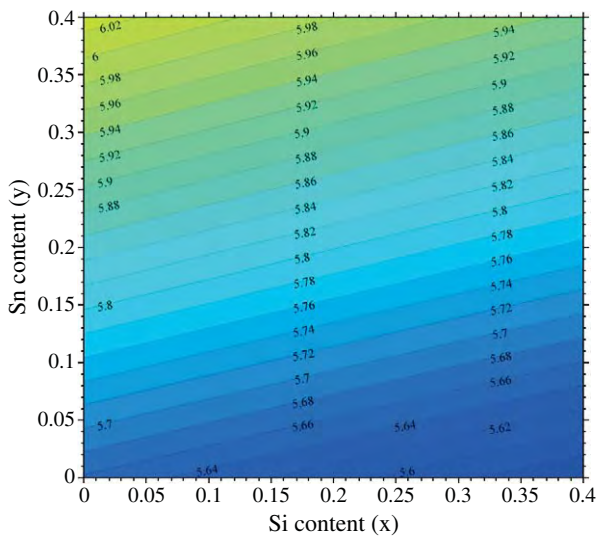

Fig. 1. The lattice constant of relaxed $Ge_{1-x-y}Si_xSn_y$ alloy calculated by Vegard's law with the bowing parameters taken into account.

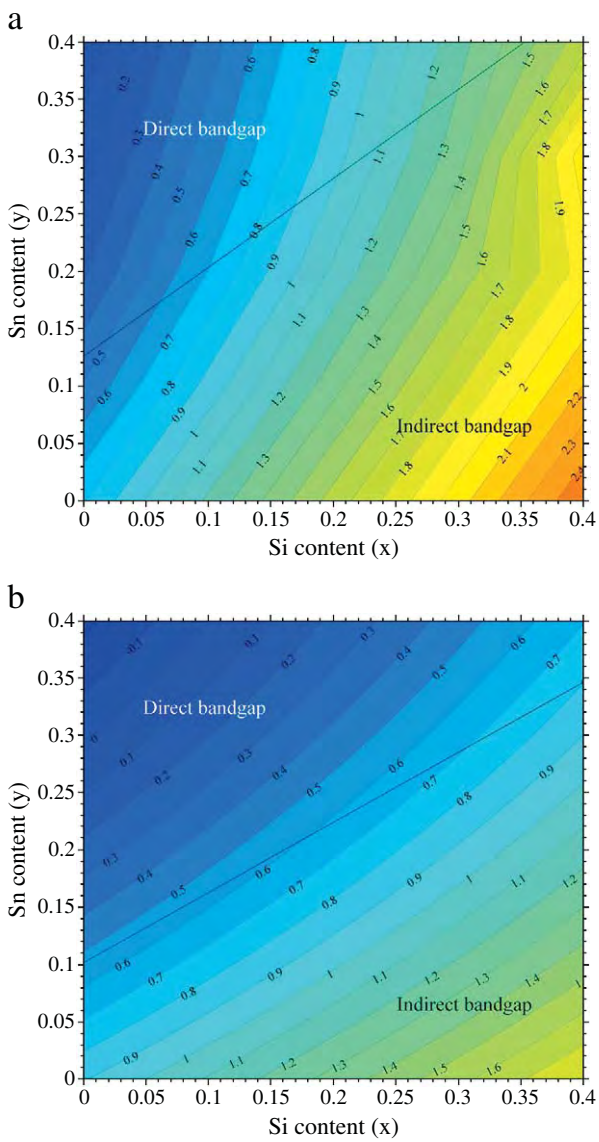

Fig. 2. The lowest (either direct or indirect) band gap of relaxed $Ge_{1-x-y}Si_xSn_y$ alloys calculated by (a) the VCA and (b) the super-cell (mixed atom) method.

to Fig. 2 which shows the band gap of the $Ge_{1-x-y}Si_xSn_y$ alloy at Γ point obtained by the two methods, only the super-cell method gives the bowing parameter in good agreement with experiment [3], where as the VCA always under estimates it.

This theoretical model was used to calculate the electronic structure of $Ge_{1-x-y}Si_xSn_y$ alloys. We find the region in the parameter space that corresponds to a direct band gap semiconductor, achieved by the material composition alone (no strain is involved here), as shown in Fig. 2. Using the data for the lattice constant (Fig. 1) and for the direct band gap (Fig. 2(b)), the strain-free direct band gap nanostructures, such as quantum wells, can be designed and fabricated by choosing two alloys with different values of the band gaps (i.e. with different composition) from the direct band gap region, but with the same lattice constants.

In particular, a strain-free $Ge_{(1-x-y)}Si_xSn_y/Ge_{(1-w)}Sn_w/Ge_{(1-x-y)}Si_xSn_y/Ge_{(1-w)}Sn_w/Ge_{(1-x-y)}Si_xSn_y$ double quantum well was designed, and its electronic structure and optical properties calculated using the effective-mass Hamiltonian model. In order to have a strain-free direct band gap nanostructure with appropriate barrier height, the $Ge_{0.75}Sn_{0.25}$ alloy was chosen as the well material and $Ge_{0.437}Si_{0.25}Sn_{0.313}$

Please cite this article as: P. Moontragoon, et al., Electronic properties calculation of $Ge_{1-x-y}Si_xSn_y$ ternary alloy and nanostructure, J. Non-Cryst. Solids (2012), doi:10.1016/j.jnoncrysol.2012.01.025

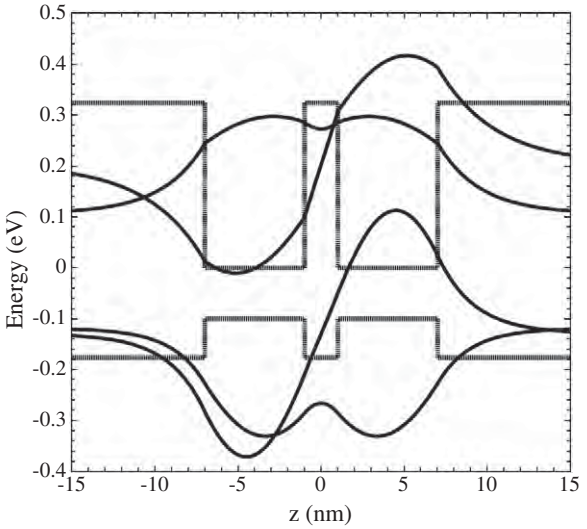

Fig. 3. The strain-free double quantum well structure $Ge_{0.437}Si_{0.25}Sn_{0.313}/Ge_{0.75}Sn_{0.25}/Ge_{0.437}Si_{0.25}Sn_{0.313}/Ge_{0.75}Sn_{0.25}/Ge_{0.437}Si_{0.25}Sn_{0.313}$ with layer widths 10/6/2/6/10 nm, and its quantized states wavefunctions (for electrons and holes).

for the barrier layers. The carrier effective masses in both layers were extracted from the electronic band structure of the two alloys, using the parabolic approximation,

$$\hbar^2/m^* = \left(\partial^2\varepsilon/\partial\mathbf{k}^2\right)$$

where m^* is the effective mass, ε the energy and **k** the wave vector. The final ingredient required for the calculations of heterostructures is the valence band offset at the interface. In the absence of any more detailed experimental data, we have used an expression in accordance to Jaros [10], i.e. for Sn grown on $Si_xGe_ySn_{(1-x-y)}$ $\Delta V_{vb} = 1.17\ x + 0.69y$ [in eV]. The band energies on the absolute energy scale are not intrinsically contained in the pseudo-potential form factors, and therefore cannot be obtained within the empirical pseudo potential method.

An example of energy levels and wave functions (electrons and holes) in a strain-free double quantum well structure $Ge_{0.437}Si_{0.25}Sn_{0.313}/Ge_{0.75}Sn_{0.25}/Ge_{0.437}Si_{0.25}Sn_{0.313}/Ge_{0.75}Sn_{0.25}/Ge_{0.437}Si_{0.25}Sn_{0.313}$ with layer widths 10/6/2/6/10 nm (i.e. based entirely on direct band gap GeSiSn materials) are shown in Fig. 3.

4. Discussion

The results indicate that only the super-cell method enables a reasonably accurate calculation of SiGeSn band structure, while the VCA should not be used (unless appropriate bowing corrections are devised for the formfunctions). However, we should note that a couple of approximations were still made in the super-cell calculation: the atomic position relaxation, due to different radii of Si, Ge, and Sn atoms, was not taken into account. Furthermore, the EPM neglects the charge transfer between different atoms due to their unequal electro-negativities, and ion core-valence electron interacting strengths. However, the ionicity and polarity in ordered SiSn and GeSn alloys are larger than in SiGe [11], but much smaller than in SiC, and that we expect that the error coming from these effects will not be large. Although these approximations will have some influence the electronic band structure of $Ge_{1-x-y}Si_xSn_y$ and heterostructures based on it, we believe that the guidelines for achieving the direct band gap, provided by the super-cell calculations presented here, will remain in place.

5. Conclusion

In search for group IV based direct band gap materials, the electronic structure of relaxed $Ge_{1-x-y}Si_xSn_y$ alloys, with x and y varying in the range 0 to 0.4, was calculated by the empirical pseudo-potential plane wave method. It shows the possibility of achieving a direct band gap semiconductor, by using appropriate compositions of silicon, germanium and tin. The results indicate that the values of the direct band gap are in the range of 0–0.8 eV, depending on the alloy composition. Therefore, this alloy can be useful for a number of electronic and optoelectronic applications, such as interband and intraband (quantum cascade) lasers, solar cells, photodetectors, electro-absorption and electro-optic modulators [12–15].

Acknowledgements

This work was financially supported by Khon Kaen University, Office of the higher education commission, and Thailand research fund.

References

[1] P. Moontragoon, Z. Ikonic, P. Harrison, Band structure calculation of SiGeSn alloy: achieving direct band gap materials, Semicond. Sci. Technol. 22 (2007) 742.
[2] R. Ragan, "Direct Energy band gap group IV Alloys and nanostructures", Dissertation, California Institute of Technology, 2005.
[3] G. He, H.A. Atwater, Interband transitions in Sn_xGe_{1-x} alloys, Phys. Rev. Lett. 79 (1997) 1937.
[4] M.V. Fischetti, S.E. Laux, Band structure, deformation potentials, and carrier mobility in strained Si, Ge, and SiGe alloys, J. Appl. Phys. 80 (1996) 2234.
[5] P. Harrison, Quantum Walls Wires and Dots: Theoretical Computational Physics, John Wiley & Sons, Chichester, 2005.
[6] A.R. Denton, N.W. Ashcroft, Vegard's law, Phys. Rev. A 43 (1991) 3161.
[7] Y. Chibane, M. Ferhat, Electronic structure of Sn_xGe_{1-x} alloys for small Sn compositions: unusual structural and electronic properties, J. Appl. Phys. 107 (2010) 053512.
[8] A. Zunger, S.-H. Wei, L.G. Ferreira, J.E. Bernard, Special quasirandom structures, Phys. Rev. Lett. 65 (1990) 353.
[9] A. Chroneos, C. Jiang, R.W. Grimes, U. Schwingenschlogl, Special quasirandom structures for binary/ternary group IV random alloys, Chem. Phys. Lett. 493 (2010) 97.
[10] M. Jaros, Simple analytic model for heterojunction band offsets, Phys. Rev. B 37 (1988) 7112.
[11] N. Amrane, S.A. Abderrahmane, H. Aourag, Band structure calculation of GeSn and SiSn, Infrared Phys. Technol. 36 (1995) 843.
[12] G. Sun, H.H. Cheng, J. Menéndez, J.B. Khurgin, R.A. Soref, Strain-free Ge/GeSiSn quantum cascade lasers based on L-valley intersubband transitions, Appl. Phys. Lett. 90 (2007) 251105.
[13] W.J. Fan, Band structures and optical gain of direct-bandgap tensile strained $Ge/Ge_{1-x-y}Si_xSn_y$ type I quantum wells, Electronic Devices, Systems and Applications (ICEDSA), 2010, p. 131.
[14] Y.-H. Zhu, Q. Xu, W.-J. Fan, J.-W. Wang, Theoretical gain of strained $GeSn_{0.02}/Ge_{1-x-y}Si_xSn_y$ quantum well laser, J. Appl. Phys. 107 (2010) 073108.
[15] P. Moontragoon, N. Vukmirovic, Z. Ikonic, P. Harrison, SnGe asymmetric quantum well electroabsorption modulators for long-wave silicon photonics, IEEE J. Select. Top. Quant. Electron. 16 (2010) 100.

Please cite this article as: P. Moontragoon, et al., Electronic properties calculation of $Ge_{1-x-y}Si_xSn_y$ ternary alloy and nanostructure, J. Non-Cryst. Solids (2012), doi:10.1016/j.jnoncrysol.2012.01.025

Ferromagnetism of C-doped CeO_2, SnO_2 and SiO_2 with oxygen vacancy diluted magnetic materials

Pairot Moontragoon[1], Anusara Jareunsheep[1], Jiranan Naosungnoen[1], Sumalee Sripho[1], Sriprajak Krongsuk[1], Ekaphan Swatsitang[1], Santi Maensiri[2]*

[1]Department of Physics, Faculty of Science, Khon Kaen University, Khon Kaen 40002, Thailand

[2]School of Physics, Suranaree University of Technology, Nakhon Ratchasima 30000, Thailand

*P. Moontragoon: Tel. +6643-203166, Fax: +6643-202374, E-mail address: mpairo@kku.ac.th

ABSTRACT Electronic structure and magnetic properties of carbon-doped cerium dioxide (CeO_2), silicon dioxide (SiO_2) and tin dioxide (SnO_2) with oxygen vacancies have been investigated by means of the first principle calculations based on local spin density approximation (LSDA), packaged in the Abinit code. The calculation was performed using self-consistent pseudo-potential plane wave. The results indicate that CeO_2, SnO_2 and SiO_2 have energy band-gap about 3.53, 2.73 and 4.21 eV respectively. For the magnatic properties of these oxides without doping and vacancy, they are antiferomagnetic materials, with zero magnetisation. However, doping carbon and the oxygen vacancies seem to play an important role for the appearance of ferromagnetism in CeO_2 but, this does not occur in the case of SnO_2 and SiO_2. These can be explained by the superexchange and double exchange theories.

Keyword- Cerium dioxide, Silicon dioxide, Tin dioxide, Diluted magnetic semiconductor

INTRODUCTION Since the discovery of ferromagnetism in a diluted magnetic semiconductor (DMS), such as Mn doped GaAs, InAs or Ge, they are continuously attracting research attention as promising spintronics semiconductors with prospective applications in semiconductor devices because of several reasons. Furthermore diluted magnetic oxides, such as CeO_2, SnO_2 and SiO_2 doped with various transition metals, such as Co, Fe, Ni and Mn[1-3], are immensely investigated, in both theory and experiment, to predict magnetic properties of these oxides which are doped with various transition metals. In this research, we studied an effect of the carbon doping and oxygen vacancy on the ferromagnetism on CeO_2, SiO_2 and SnO_2.

COMPUTATIONAL DETAILS Electronic and magnetic properties for C-doped cerium oxide (CeO_{2-x}), silicon dioxide (SiO_{2-x}) and tin oxide (SnO_{2-x}) with oxygen vacancies have been investigated by first principle methods using the Abinit code. The calculation was performed using self-consistent pseudo-potential plane wave with LSDA formalism to explore the possibility of ferromagnetism as observed in recent experiments[2-3]. The carbon-doped, cerium oxide, silicon dioxide and tin dioxide with oxygen vacancies were modeled using a 1×1×1 supercell in ideal fluorite structure (12 atoms), a 1×1×2 alpha quartz structure (18 atoms) and a 1×1×2 rutile structure (12 atoms) respectively, without structural optimization, as shown in Fig 1. A 8×8×8, 8×8×4 and 8×8×4 Monkhorst-Pack k–point mesh was used for the cerium, silcon dioxide and tin dioxide super cell calculation, respectively. A plane wave with cutoff energy of 14 Hartree was used to assure convergent results.

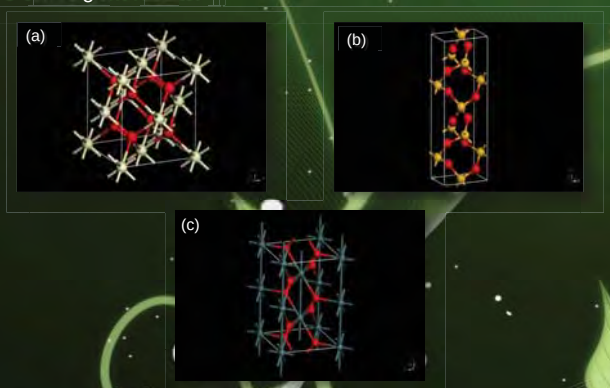

FIG. 1 The crystal structures of (a) pure cerium oxide when red represent O atoms and gray represent Ce atoms (b) pure quartz silicon dioxide when red represent O atoms and yellow represent Si atoms, and (c) pure tin dioxide when red represent O atoms and dark green represent Sn atoms.

ACKNOWLEGEMENT This work was financially supported by Khon Kaen University, Office of the higher education commission, and Thailand research fund.

REFERENCES

[1]Andersson D. A, Simak, S. I, Skorodummova N. V, Abrikosov I. A. and B. Johansson, "Theoretical study of CeO_2 doped with trivalent ions" *Phys. Rev. B.* 76, 174119 (2007)

[2]Maensiri S., Phokha S., Laokul P., and S. Seraphin; "Room Temperature Ferromagnetism in Fe-Doped CeO_2 Nanoparticles" *J. Nanosci. Nanotechnol* 9, 1-6 (2009)

[3]Vodungbo B., Zheng Y., Vidal F., Etgens V. H. and D. H. Mosca; "Room temperature ferromagnetism of Co doped CeO_{2-x} diluted magnetic oxide: Effect of oxygen and anisotropy" *Appl. Phys. Lett.* 90, 062510 (2007)

RESULTS AND DISCUSSION

Electronic property

According to the total density of states (DOS), shown in Fig. 4, calculated by LSDA, it indicates that CeO_2 has energy band-gap about 3.53 eV, which is in good agreement with the other calculation [5]. However, the energy band gap is still under-estimated when compared with the experiment value, due to local density approximation. There are also states occurring between the conduction band and the valence band (intermediate band) when doped with carbon and oxygen vaccancy. Like the density of states of cerium oxide, DOS of silicon dioxide also has intermediate bands when doped with carbon atom, as shown in Fig. 4. The energy band gap of pure quartz silicon dioxide is about 4.21 eV and about 2.73 eV for pure tin dioxide.

Magnetic property

The magnetic properties of the C-doped CeO_{2-x}, SnO_{2-x} and SiO_{2-x} and the effect of oxygen vacancies are described as follows. According to the LSDA calculation, the magnetisation of CeO_2, CeO_2 with oxygen vacancy and C-doped CeO_2 has magnetic moments of zero, 2.16 and 1.94 μ_B, respectively. In the case of pure cerium and C-doped, this can be explained by using superexchange theory, i.e. the two unpair electrons in the 4d orbital have interaction between two next-to-nearest neighbor cations, Ce atoms, through a non-magnetic anion, O atom with valence electrons in 2p orbital (spin up and spin down), as shown in Fig 2(a). Therefore, the total net spin of pure cerium is 0, but not in C-doped CeO_2.

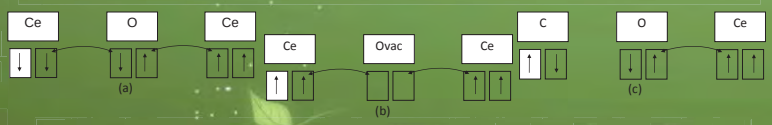

FIG. 2 The electron configurations and interaction of (a) pure CeO_2 (b) CeO_{2-x} with oxygen vacancy and (c) C-doepd CeO_2.

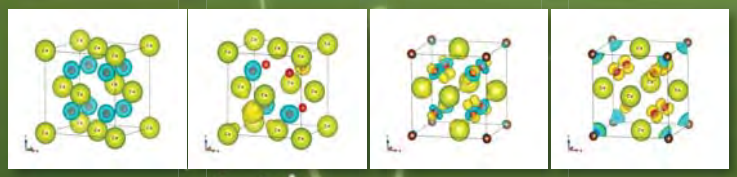

FIG. 3 The isosurface of difference between spin up electron density and spin down electron density (spin up – spin down) of (a) pure CeO_2, (b) with oxygen vacancy, (c) C-doped CeO_2, and (d) C-doped CeO_{2-x} with oxygen vacancy.

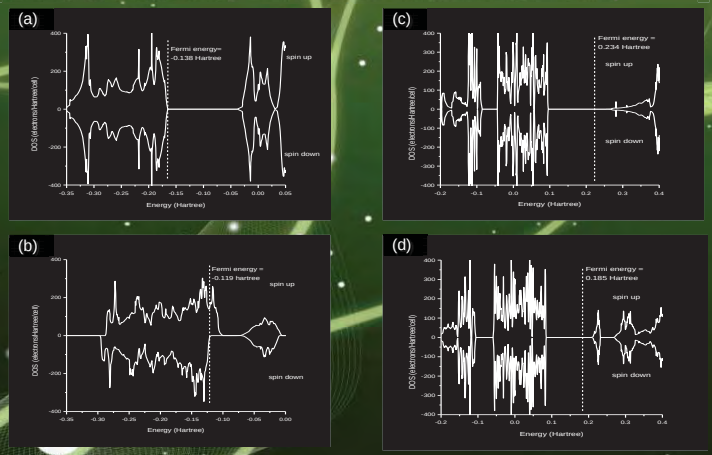

FIG. 4 Total density of states (DOS) of (a) pure cerium dioxide, (b) C-doped cerium dioxide, (c) pure silicon dioxide, and (d) C-doped silicon dioxide

CONCLUSION Electronic structure and magnetic properties for carbon-doped cerium oxide, silicon dioxide and tin oxide with oxygen vacancy have been investigated by means of the first principle calculations based on local spin density approximation (LSDA) scheme, packaged in the Abinit code. The results indicate that cerium dioxide, tin dioxide and silicon dioxide are a wide-gap semiconductor and the carbon-doped and oxygen vacancies play important role in magnetic behavior of CeO_2, but do not in silicon dioxide and tin oxide. There are also intermediate band in CeO_2 and SiO_2 when doped with carbon or oxygen was removed.

Electronic properties calculation of $Ge_{1-x-y}Si_xSn_y$ ternary alloy nanostructure

Pichitpon Pengpit[1], Pairot Moontragoon[*, 1], Thanusit Burinprakhon[1], Santi Maensiri[2], Nenad Vukmirovic[3], Zoran Ikonic[4] and Paul Harrison[4]

[1] Department of Physics, Faculty of Science, Khon kaen University, Khon kaen, 40002, Thailand
[2]School of Physics, Suranaree University of Technology, Nakhon Ratchasima 30000, Thailand
[3] Institute of Physics, University of Belgrade, Serbia, Yugoslavia
[4] School of Electronic and Electrical Engineering, University of Leeds, Leeds, United Kingdom
*e-mail: mpairo@kku.ac.th

ABSTRACT The band structure of $Ge_{1-x-y}Si_xSn_y$ ternary alloys, which are easier to grow than $Ge_{1-x}Sn_x$ alloys only, and clearly offer a wider tunability of their direct band-gap and properties, was calculated and investigated by using the empirical pseudo-potential plane wave method with classical Falicov pseudo-potential form. The virtual crystal approximation was adopted to model the alloy. In order to calculate all of these properties, the empirical pseudo-potential code was developed. According to the results, lattice constant of alloy varies from 5.4 to 6.4 Angstrom. The region in the parameter space that corresponds to a direct and indirect band gap semiconductor was displayed. The $Ge_{1-x-y}Si_xSn_y$ ternary alloy shows the direct band gap semiconductor for appropriated concentration of Si, Ge and Sn. The direct energy gap of the alloy is in the rage of 0-1.3 eV, depending on the amount of Si , Ge and Sn doped. Thus, the alloy is a promising material for optoelectronic applications in both visible and infrared range, such as interband lasers, solar cell.

Keyword *Silicon photonic devices, SiGeSn alloys, Direct band gap semiconductor*

INTRODUCTION SiGeSn alloys have attracted research attention as promising materials for optoelectronic applications, such as interband lasers and detectors, solar cells, because they possibly are direct bandgap semiconductor, and highly compatible with Si-based technology. They have the potential for independent variation of the band structure and lattice constant and can be used in both lattice-matched and strained layer structures. Offering the possibility of emission and absorption in the visible, near- and mid-IR range, they have the prospect of applications for interband and intraband (quantum cascade) lasers, solar cell, photodetectors, electro-absorption and electro-optic modulators, etc.

COMPUTATIONAL DETAILS For band structure calculation of $Ge_{1-x-y}Si_xSn_y$ alloys, we use the empirical pseudo-potential plane wave method and the alloys were modeled by the virtual crystal approximation method (VCA), using the available experimental data for comparison. The classical Falicov pseudo-potential form was adopted.

$$V(q)=\frac{1}{2}\frac{a_1\left(q^2-a_2\right)}{1+e^{a_3\left(q^2-a_4\right)}}\left[\tanh\left(\frac{a_5-q^2}{a_6}\right)+1\right]$$

with the parameters which shown in Table 1 and **q** is wave vector.

Parameter	a_1	a_2	a_3	a_4	a_5	a_6
Si	0.3969	2.2286	0.6120	-1.9620	5.0	0.3
Ge	0.4229	2.4682	0.6060	-2.6260	5.0	0.3
α-Sn	0.4199	2.1600	0.6407	-2.9820	5.0	0.3

Table 1. The parameters for the classical Falicov pseudo-potential of silicon, germanium and gray tin

RESULTS AND DISCUSSION

From the Fig. 1 (a) The lattice constant of $Ge_{1-x-y}Si_xSn_y$ alloy was calculated by using the Vergard law. The lattice constant of alloy was approximated by using linearly Interpolation of lattice constant of silicon, germanium and alpha tin.

Band structure calculations of SiGeSn alloys: achieving direct band gap materials

We describe the theoretical model used to calculate the electronic structure of $Ge_{1-x-y}Si_xSn_y$ alloy. We find the region in the parameter space that corresponds to a direct band gap semiconductor, achieved by the combined influence of material composition and strain, as showed in Fig. 2(c). According to the information about lattice constant (Fig. 1 (a)) and the direct band gap region (Fig. 1 (d)), the unstrained direct band gap nanostructure, such as quantum wells, can be fabricated by choosing two alloys with different band gap (different silicon, germanium and tin composition) in the direct band gap region but it still have the same lattice constant.

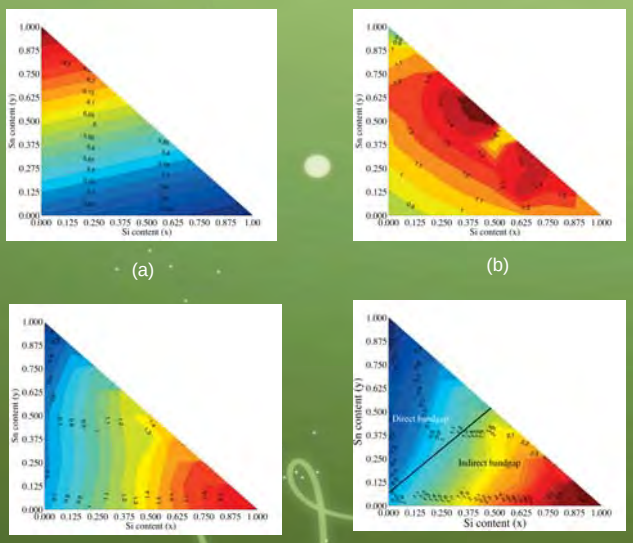

Fig. 1 (a) The lattice constant of relaxed $Ge_{1-x}Sn_x$ calculated by Vergard law and The energy band gap of $Ge_{1-x-y}Si_xSn_y$ alloy at (b) X valley (c) L valley and (d) Γ point

CONCLUSION In search for direct gap materials, the electronic structure of relaxed $Ge_{1-x}Sn_x$ alloys was calculated by the empirical pseudo-potential plane wave method. It shows an achieving a direct band gap semiconductor, by using appropriate composition of silicon, germanium and gray tin . The results show that the direct energy gap of are in the rage of 0-1.3 eV, depending on the amount of Si , Ge and Sn doped. Therefore, the alloy can be used as material for many electronic applications, such as lasers, solar cell, photodetectors, electro-absorption and electro-optic modulators.

ACKNOWLEGEMENT This work was financially supported by Khon Kaen University, Office of the higher education commission, and Thailand research fund.

REFERENCES

[1] G. He and H. A. Atwater, Phys. Rev. Lett. 79, 1937 (1997)
[2] P. Moontragoon, N. Vukmirovic, Z. Ikonic, and P. Harrison, Journal of Applied Physics 103, 103712 (2008)
[3] G. Sun, H. H. Cheng, J. Menéndez, J. B. Khurgin, and R. A. Soref, Applied Physics Letters 90, 251105 (2007)
[4] P. Moontragoon, Z. Ikonić, and P. Harrison, "Band structure calculations of SiGeSn alloys: achieving direct band gap materials", *Semicond. Sci. Technol.* 22, 742 (2007).